

DESY 00-036
 KA-TP-4-2000
 UAB-FT-483
 UG-FT-113/00
 hep-ph/0003109

Top-Quark Production and Decay in the MSSM¹

J. GUASCH^a, W. HOLLIK^a, J.I. ILLANA^{b,c}, C. SCHAPPACHER^a, J. SOLÀ^d

^a Institut für Theoretische Physik, Universität Karlsruhe, D-76128 Karlsruhe, Germany

^b DESY, Platanenallee 6, D-15738 Zeuthen, Germany

^c Dpto. Física Teórica y del Cosmos, Universidad de Granada, E-18071 Granada, Spain

^d Grup de Física Teòrica and Institut de Física d'Altes Energies, Universitat Autònoma de Barcelona, E-08193 Bellaterra (Barcelona), Catalonia, Spain

Abstract

We review the features of top-quark decays and loop-induced effects in the production cross section and CP-violating observables of $e^+e^- \rightarrow t\bar{t}$ which are specific to the R -parity conserving Minimal Supersymmetric Standard Model (MSSM).

¹Contribution to the proceedings of the 2nd Joint ECFA/DESY Workshop on *Physics and Detectors for a Linear Electron-Positron Collider*, based on talks presented by J.I. Illana at Frascati (Italy) November 8-10th 1998, J. Guasch at Oxford (UK) March 20-23 1999 and W. Hollik at Obernai (France) 16-19th October 1999.

1 Introduction

The Standard Model (SM) of strong (QCD) and electroweak (EW) interactions has been the most successful framework to describe the phenomenology of high energy physics. However, one of the fundamental building blocks (the Higgs boson) still lacks experimental confirmation. On the other hand, the SM still suffers from some theoretical deficiencies, most notably the hierarchy problem. Several extensions of the SM have been proposed to solve these problems; in this note we will concentrate on its supersymmetric (SUSY) extension, more specifically to the R -parity conserving Minimal Supersymmetric Standard Model (MSSM) [1].

The top quark, due to its large mass, could play a central role in the search of physics beyond the SM. On one hand it could decay to non-standard particles, on the other hand, due to its large Yukawa coupling, the effects of the Spontaneous Symmetry Breaking Sector are expected to be larger than for any other particle of the model. In the MSSM, these effects are reinforced by the presence of the SUSY partners of the top quark and Higgs bosons. Moreover, the new parameters appearing in the MSSM can have complex phases, and new sources of CP-violation phenomena can appear.

One should also bear in mind that, before the commissioning of TESLA, the LHC will be producing data which might turn out to include some physics beyond the SM, and we must be prepared for whatever the high energy physics scenario would be for the running of TESLA.

Here we present a review of the effects of SUSY in the top-quark phenomenology. First we review in section 2 the top-quark decay within the framework of the MSSM; then, in section 3, we present the MSSM effects on the top quark pair production in e^+e^- collisions, both in the presence and absence of CP-violating couplings.

2 Top-quark decays

The existence of SUSY could affect the total top-quark decay width in two ways. First of all through unexpected radiative corrections to the standard top quark decay process $t \rightarrow W^+ b$. Second, some of the SUSY particles could be lighter than the top quark itself, thus providing new channels in which the top quark could decay.

Concerning the standard top-quark decay, we point out that its branching ratio $\text{BR}(t \rightarrow W^+ b)$ is not so severely constrained by the observed top quark production cross section as one could naively think at first sight [2]. In the MSSM the total observed cross section can be written, schematically, as

$$\begin{aligned} \sigma_{\text{obs}} = & \int dq d\bar{q} \sigma(q\bar{q} \rightarrow t\bar{t}) \times |\text{BR}(t \rightarrow W^+ b)|^2 \\ & + \int dq d\bar{q} \sigma(q\bar{q} \rightarrow \tilde{g}\tilde{g}) \times |\text{BR}(\tilde{g} \rightarrow t\bar{t}_1)|^2 \times |\text{BR}(t \rightarrow W^+ b)|^2 \\ & + \int dq d\bar{q} \sigma(q\bar{q} \rightarrow \tilde{b}_a\tilde{b}_a) \times |\text{BR}(\tilde{b}_a \rightarrow t\chi_1^-)|^2 \times |\text{BR}(t \rightarrow W^+ b)|^2 + \dots \end{aligned} \quad (1)$$

Here $\int dq$ represents the integration over the quarks Parton Distribution Functions, and summation over quark flavours. In the SM only the first line of this equation is present. It follows that, in the MSSM, our present ignorance of the SUSY parameters prevents us from performing a detailed calculation of the $t\bar{t}$ production cross section as well as

from putting a strict limit on $\text{BR}(t \rightarrow \text{"new"})$ — the branching ratio of the top quark into new physics. It should also be clear that the observed cross section in Eqn. (1) refers not only to the standard $bW bW$ events, but to all kind of final states that can mimic them. Thus, effectively, we should substitute $\text{BR}(t \rightarrow X b)$ in that formula for $\text{BR}(t \rightarrow W^+ b)$, and then sum the cross section over X , where X is any state that leads to an observed pattern of leptons and jets similar to those resulting from W -decay. In particular, $X = H^\pm$ would contribute (see below) to the τ -lepton signature, if $\tan\beta$ is large enough. Similarly, there can be direct top quark decays into SUSY particles that could mimic the SM decay of the top quark [3]. The only restriction is an approximate lower bound $\text{BR}(t \rightarrow W^+ b) \gtrsim 40 - 50\%$ in order to guarantee the purported standard top quark events at the Tevatron [4]. Thus, from these considerations it is not excluded that the non-SM branching ratio of the top quark, $\text{BR}(t \rightarrow \text{"new"})$, could be comparable to the SM one — or at least not necessarily much smaller.

The e^+e^- Linear Collider (LC) provides an excellent tool to test the various top quark partial decays widths. The total top quark decay width can be measured by means of a threshold scan, in a model independent way [5]. Also the clean environment allows for a high prospect for detecting exclusive rare decay channels.

2.1 The top-quark standard decay width

In the SM the top-quark decays into a W^+ gauge boson and a bottom quark. The tree-level prediction for this partial decay width is (for $m_t = 175 \text{ GeV}$)

$$\begin{aligned} \Gamma_{\text{SM}}^0(t \rightarrow W^+ b) &= \left(\frac{G_F}{8\pi\sqrt{2}} \right) \frac{|V_{tb}|^2}{m_t} \lambda^{1/2}(1, m_b^2/m_t^2, M_W^2/m_t^2) \\ &\times [M_W^2(m_t^2 + m_b^2) + (m_t^2 - m_b^2)^2 - 2M_W^4] \simeq 1.55 \text{ GeV} \end{aligned} \quad (2)$$

where $\lambda^{1/2}(1, x^2, y^2)$ is the usual Källen function. As the width turns out to be much larger than the typical scale of non-perturbative QCD effects Λ_{QCD} , it can be conceived as an effective infrared cut-off. This means that the top quark, due to its large mass, has time to weakly decay before strong hadronization processes come into play. And for this reason perturbative computations in top quark physics are reliable.

In this spirit the SM quantum corrections to the standard top quark decay width have been performed. The short-distance QCD effects have been computed up to two-loop level [6, 7] and they amount to a correction of -10% with respect to the tree-level width. The electroweak (EW) SM radiative correction is also available [7, 8], but this contribution is below $+2\%$ in a scheme where the tree-level width is parametrized in terms of the Fermi constant G_F — as in Eqn.(2). In this scheme the electroweak corrections are minimized both in the SM and in the MSSM because the set of universal contributions — viz. those encoded in the parameter Δr — cancel out.

The MSSM may furnish extra (perturbative) quantum effects on the standard decay width of the top quark through the one-loop corrections mediated by non-SM particles. They have been computed in [9, 10]² and can be of two types, electroweak and strong.

²The corresponding corrections in the general 2HDM can be found in Refs. [11, 12]. The particularization of these Higgs effects in the MSSM is studied in [11].

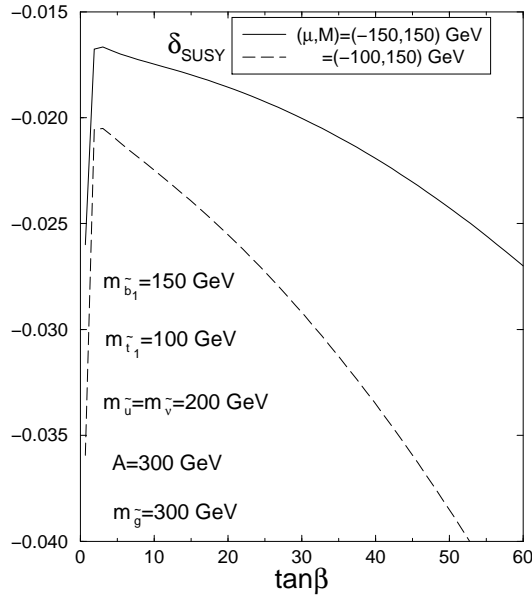


Figure 1: The total (electroweak and strong) SUSY correction to $\Gamma(t \rightarrow W^+ b)$ for given sets of parameters and $m_t = 175$ GeV.

The SUSY-EW quantum corrections [9] are negative (as the standard QCD ones) and vary from -1% to -10% , depending on the choice of the various SUSY parameters, and, especially of $\tan\beta$. The corrections due to additional Higgs particle exchange (i.e. the MSSM Higgs effects after subtracting the corresponding SM limit of the MSSM Higgs sector) are at most of 0.1% due to the severe constraints that SUSY imposes on the MSSM Higgs sector.

The SUSY-QCD corrections, mediated by gluinos and squarks, have also been found to be negative in most of the parameter space [10], though they are in general smaller than the SUSY-EW ones — namely, around a few % level — and they are independent of $\tan\beta$.

In Fig. 1 we show the total SUSY (electroweak and QCD) corrections to this decay width for typical values of the SUSY spectrum. The upshot is that the total SUSY corrections to $\Gamma(t \rightarrow W^+ b)$ go in the same direction as the standard QCD ones. For large values of $\tan\beta$ they can typically yield an effect about half the size of the QCD corrections, thus providing an additional (potentially measurable) decrease of the tree-level value of the standard width (2).

2.2 Top-quark decay into charged Higgs

If the charged Higgs is light enough the top quark will also decay through the process $t \rightarrow H^+ b$. This decay has been subject of interest since very early in the literature [13]. If $\tan\beta$ is large or small enough the tree-level prediction for the partial decay width $\Gamma^0(t \rightarrow H^+ b)$ is comparable to the standard one (2). In fact $\Gamma^0(t \rightarrow H^+ b)$ presents a minimum at the point $\tan\beta = \sqrt{m_t/m_b} \simeq 6$ and grows for larger or smaller values of $\tan\beta$ (see Fig. 2). Remarkably enough, this process turns out to be extremely sensitive to

radiative corrections of all kinds. On one hand, the standard QCD corrections are quite large. They are negative and for $\tan\beta \gtrsim 10$ they saturate around the value -58% [14]. On the other hand, the full set of the MSSM radiative corrections, at the one-loop level, can also be very important. They have been computed in [15–17], and more recently the general 2HDM corrections became also available [18].

In the case of the EW corrections one needs to define renormalization prescriptions also for the non-SM parameters that appear in these decays, in particular for the highly relevant parameter $\tan\beta$. The renormalization counterterm for $\tan\beta$ can be fixed in many different ways. The actual corrections will depend on the particular definition, but not so the value of the physical observable, of course. In our case we found it practical to define $\tan\beta$ through the condition that the partial decay width $\Gamma(H^+ \rightarrow \tau^+ \nu_\tau)$ does not receive radiative corrections. This is a good choice for the scenario under study, since this is the dominant decay of a light charged Higgs boson (i.e. $M_{H^\pm} < m_t$) provided $\tan\beta$ is of order 1 or above: $\tan\beta > \sqrt{m_c/m_s} \gtrsim 2$. Under this renormalization prescription, and for moderate or large $\tan\beta \gtrsim 10$, the bulk of the SUSY quantum corrections are known to stem from the finite threshold corrections to the bottom mass counterterm. The relevant effects are triggered by R -odd particles entering the bottom self-energy, and can be cast as follows [16, 17]

$$\begin{aligned}
\left(\frac{\delta m_b}{m_b} \right)_{S-QCD} &= \frac{2\alpha_s(m_t)}{3\pi} m_{\tilde{g}} M_{LR}^b I(m_{\tilde{b}_1}, m_{\tilde{b}_2}, m_{\tilde{g}}) \\
&\rightarrow -\frac{2\alpha_s(m_t)}{3\pi} m_{\tilde{g}} \mu \tan\beta I(m_{\tilde{b}_1}, m_{\tilde{b}_2}, m_{\tilde{g}}), \\
\left(\frac{\delta m_b}{m_b} \right)_{S-EW} &= -\frac{h_t h_b}{16\pi^2} \frac{\mu}{m_b} m_t M_{LR}^t I(m_{\tilde{t}_1}, m_{\tilde{t}_2}, \mu) \\
&\rightarrow -\frac{h_t^2}{16\pi^2} \mu A_t \tan\beta I(m_{\tilde{t}_1}, m_{\tilde{t}_2}, \mu), \\
I(m_1, m_2, m_3) &\equiv 16\pi^2 i C_0(0, 0, m_1, m_2, m_3) \\
&= \frac{m_1^2 m_2^2 \ln \frac{m_1^2}{m_2^2} + m_2^2 m_3^2 \ln \frac{m_2^2}{m_3^2} + m_1^2 m_3^2 \ln \frac{m_3^2}{m_1^2}}{(m_1^2 - m_2^2)(m_2^2 - m_3^2)(m_1^2 - m_3^2)}, \tag{3}
\end{aligned}$$

where C_0 is the three-point 't Hooft-Passarino-Veltman function [19], and the rightmost expressions hold for sufficiently large $\tan\beta$. Several important consequences can be derived already from the approximate expressions (3). The first one corresponds to the sign of the corrections. The sign of the SUSY-QCD corrections is opposite to that of the higgsino mass parameter μ , whereas the sign of the SUSY-EW corrections is given by the product of μ and the soft-SUSY-breaking trilinear coupling A_t . Second, both kind of corrections grow linearly with $\tan\beta$. A third, and important, observation is that, if we scale all the dimensionful parameters of Eqn. (3) by a factor λ , the λ -dependence drops out in the final expression. This means that raising the scale of SUSY breaking does not reduce the effects of the radiative corrections. Notice, however, that this consideration amounts to scale up also the trilinear coupling A_t as well as the higgsino parameter μ . Therefore, it may lead to unwanted fine-tuning effects in at least two important sectors

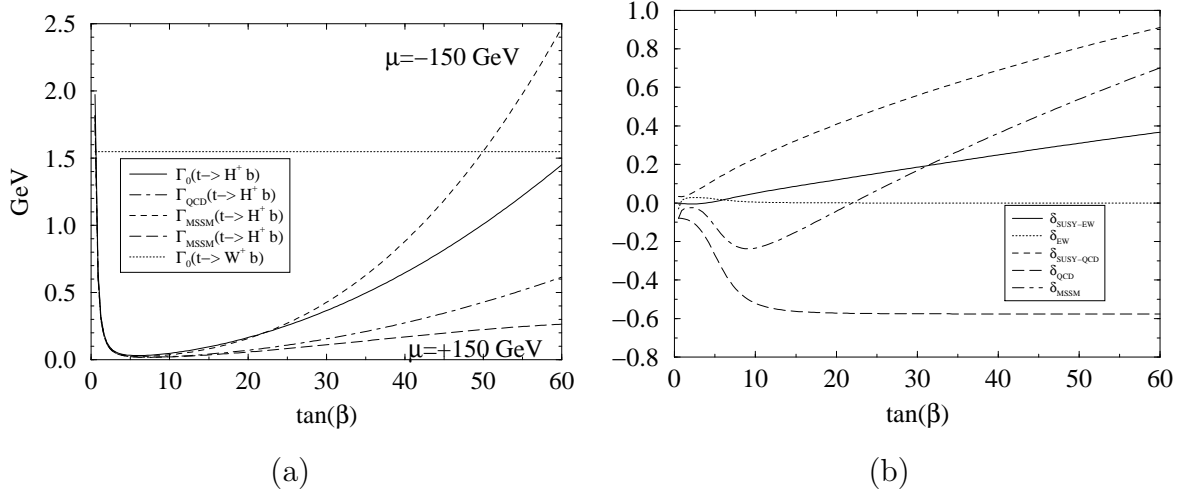


Figure 2: **(a)** The top-quark partial decay width $\Gamma(t \rightarrow H^+ b)$ compared with the standard one as a function of $\tan \beta$, and for $M_{H^\pm} = 120$ GeV. Shown are the tree-level width, the QCD corrected width, and the full MSSM corrected width for two sets of the SUSY parameters A : $\{\mu, m_{\tilde{t}_1}, m_{\tilde{b}_1}, m_{\tilde{g}}, A_t\} = \{-150, 100, 150, 300, +300\}$ GeV $B: \{+150, 200, 600, 1000, -300\}$ GeV. **(b)** The relative radiative corrections to $\Gamma(t \rightarrow H^+ b)$ for each of the sectors of the MSSM (A parameter set).

of the MSSM: in the Higgs and squark sectors. Notwithstanding, if one does not stretch out the ranges of the parameters up to unreasonable limits (i.e. much beyond 1 TeV or so), an important consequence can be derived without disrupting the natural structure of the model, to wit: that the R -odd particles whose masses are above the EW scale can effectively display, in the presence of Yukawa couplings, a non-decoupling behaviour. And this behaviour is triggered by the existence of explicit soft SUSY-breaking terms in combination with the spontaneous breaking of the gauge symmetry. Obviously, this is a very important feature as it could produce visible radiative corrections for this decay.³ Recently these finite threshold effects have been further refined in the literature and they have been re-summed to all orders [21].

In the case of the gluino mass dependence there is another trait that we wish to remark. Even without scaling up the rest of the SUSY parameters, the SUSY-QCD corrections to $\Gamma^0(t \rightarrow H^+ b)$ exhibit a local, and lengthy sustained, maximum around $m_{\tilde{g}} \gtrsim 300$ GeV. Only for gluino masses well above the TeV scale (for fixed values of the squark masses) do these corrections eventually decouple [16]. As for the corrections due to Higgs bosons loops, of which there are quite a few, we find that they are entirely negligible compared to the yield from R -odd particles.⁴

Figure 2a presents a summary of the main results. Here we have plotted the partial decay width $\Gamma(t \rightarrow H^+ b)$ as a function of $\tan \beta$, for the two different scenarios that have been identified. In the first one ($\mu < 0$) the SUSY-QCD corrections are opposite in sign to the QCD ones, thus canceling partially (or even totally) the SM strong corrections. In the

³We should like to say that this feature is not limited to just the high energy process under consideration, but it applies equally well to some low-energy processes, e.g. in B-meson decays [20].

⁴This effect is due to the restrictions that SUSY imposes to the form of the Higgs bosons potential. In the unrestricted 2HDM the Higgs bosons loop corrections can also be important [18].

second one ($\mu > 0$) the SUSY-QCD corrections have the same sign as the standard QCD ones, so reinforcing the large negative corrections. In both cases we have fixed $\mu A_t < 0$, which is the overall sign which makes allowance for the low energy data on radiative B meson decays to be compatible with the existence of a light charged Higgs below the top quark mass [22]. This fixes the SUSY-EW corrections (3) to be positive. In Fig. 2b we present the relative corrections induced by each sector of the MSSM, in the $\mu < 0$ scenario.

The results shown in Fig. 2 can hardly be overemphasized. Whereas the QCD prediction for the partial decay width states that this is always significantly smaller than the standard partial decay width, in the $\mu < 0$ scenario the charged Higgs partial decay width is equal to the standard one for $\tan\beta \simeq 50$, and it is rapidly increasing. In this scenario the presence of charged Higgs in top quark decays is significantly greater than the QCD prediction, and thus the experimental discovery reach of charged Higgs in top quark decays can be larger than expected. On the other hand in the $\mu > 0$ scenario the discovery reach is decreased with respect to the standard one. Thus the excluded region in the $\tan\beta - M_{H^\pm}$ plane due to the (up to now) unsuccessful search of charged Higgs bosons in top quark decays depends drastically on the value of the rest of parameters in the MSSM [23].

In Fig. 2b we see clearly the close-to-linear behaviour of the leading SUSY contributions (3), and we also see that the Higgs-boson mediated contributions (δ_{EW} in the plot) really play a marginal role. Interestingly enough we see that for $\tan\beta \simeq 35$ the SUSY-QCD corrections cancel the standard QCD ones, and thus, although the larger corrections are due to the strong interaction sector, the only radiative corrections that are left are the SUSY-EW ones.

The SUSY radiative corrections above $\tan\beta \simeq 35$ (at one-loop) can easily reach values of

$$\begin{aligned} \delta_{S-EW} &\simeq +30\% , \quad \delta_{S-QCD} \simeq +80\% \quad (\mu < 0, A_t > 0, M_{SUSY} \simeq 100 - 200 \text{ GeV}) , \\ \delta_{S-EW} &\simeq +20\% , \quad \delta_{S-QCD} \simeq -40\% \quad (\mu > 0, A_t < 0, M_{SUSY} \simeq 500 \text{ GeV}) . \end{aligned} \quad (4)$$

Negative corrections for the SUSY-EW corrections of the same absolute values are possible provided $\mu A_t > 0$. We have singled out different sparticle spectra for the two scenarios in order to avoid total corrections greater than 100% when they are added to the standard QCD corrections.

2.3 FCNC top-quark decays

Flavour Changing Neutral Current (FCNC) decays of the top quark are one-loop induced processes. They are such rare events in the SM [24], with branching ratios at the level of $10^{-10} - 10^{-15}$ depending on the particular channel, that its presence at detectable levels would clearly indicate the presence of new physics. The question is whether the presence of SUSY particles could enhance these partial decay widths up to the visible level. The partial FCNC decay width into a weak vector boson $\Gamma(t \rightarrow cV)$ ($V = Z, \gamma$) undergoes some enhancement [25, 26], however it is still of the order of $10^{-12} - 10^{-13}$ in most of the parameter space, thus being far away of the detection level. The gluon channel ($t \rightarrow cg$) is

the most gifted one in the SM, but it is nevertheless too small to be detectable ($\sim 10^{-10}$). This mode, however, has recently been analyzed in great detail in the MSSM [26–28] and one finds that its branching ratio can be close to the visible threshold for the future high luminosity machines such as the LHC and the LC (see below). Finally, the top quark decaying into neutral Higgs particles ($t \rightarrow ch$, $h = h^0, H^0, A^0$) has also been shown to benefit from large enhancements in the MSSM framework [27–29]. In this respect we recall that in the MSSM the channel in which the lightest Higgs boson is involved ($t \rightarrow ch^0$) is always kinematically open because $m_{h^0} \leq 130 \text{ GeV} < m_t$. Hereafter we will concentrate on the two decays, $t \rightarrow cg$ and $t \rightarrow ch^0$, because the overall analysis shows that they are the most efficient FCNC decays in their respective modalities. Of course in SUSY models beyond the MSSM, such as models without R -parity, there could be other kind of competing FCNC top quark decays,⁵ but here we shall stick all the time to the MSSM.

FCNC processes can be induced through SUSY-EW charged current interactions. These proceed through the same mixing matrix elements as in the SM: the Cabibbo-Kobayashi-Maskawa mixing matrix. But in addition it could happen that the squark mass matrix squared is not proportional to the quark-mass-matrix squared. In this case the squark mass eigenstates would not coincide with the quark mass states, and as a consequence tree-level FCNC would appear in the quark-squark-gaugino/higgsino interactions. This mixing appears as non-flavour diagonal mass matrix elements in the squark mass matrix squared

$$(M_{LL}^2)_{ij} = m_{ij}^2 \equiv \delta_{ij} m_i m_j, \quad (i \neq j), \quad (5)$$

where i, j represent squarks of any generation, and $m_{\{i,j\}}$ is the mass corresponding to the diagonal entries in the matrix. In the MSSM these kind of mixing terms in the Left-chiral sector are naturally generated through the Renormalization Group evolution of the soft-SUSY-breaking squark masses down to the EW scale [31]. This is the reason why we just singled out the LL mixing component in Eqn. (5). Flavour mass mixing terms for the corresponding Right-chiral squarks are allowed, but they do not appear naturally in the GUT frameworks. Moreover its presence is not essential because it does not change the order of magnitude of the results obtained with only flavour-mixing between Left-chiral squarks [26, 27]. The mixing terms δ_{ij} are restricted by the low energy data on FCNC processes [32]. These limits were computed using the mass-insertion approximation, so they should be taken as order of magnitude limits. Recently it has been shown that the full computation of some FCNC process can give results which differ substantially from the mass-insertion approximation ones [33].

To assess the size of the FCNC top quark decay rates we use the fiducial ratio

$$B(t \rightarrow ch) \equiv \frac{\Gamma(t \rightarrow c X)}{\Gamma(t \rightarrow b W^+)}, \quad (6)$$

for both $X = g, h^0$. The typical values of this ratio lie in the ballpark of 10^{-8} for the SUSY-EW contributions in the regime of large $\tan \beta$ ($30 \lesssim \tan \beta \lesssim 50$) and for a SUSY spectrum around 200 GeV. This is already five orders of magnitude larger than the corresponding processes in the SM. The SUSY-QCD contributions, which appear when the δ_{23} in Eqn. (5) is non-zero for up-type squarks, are typically around two orders of

⁵See e.g. Refs. [30] for some recent works on the subject.

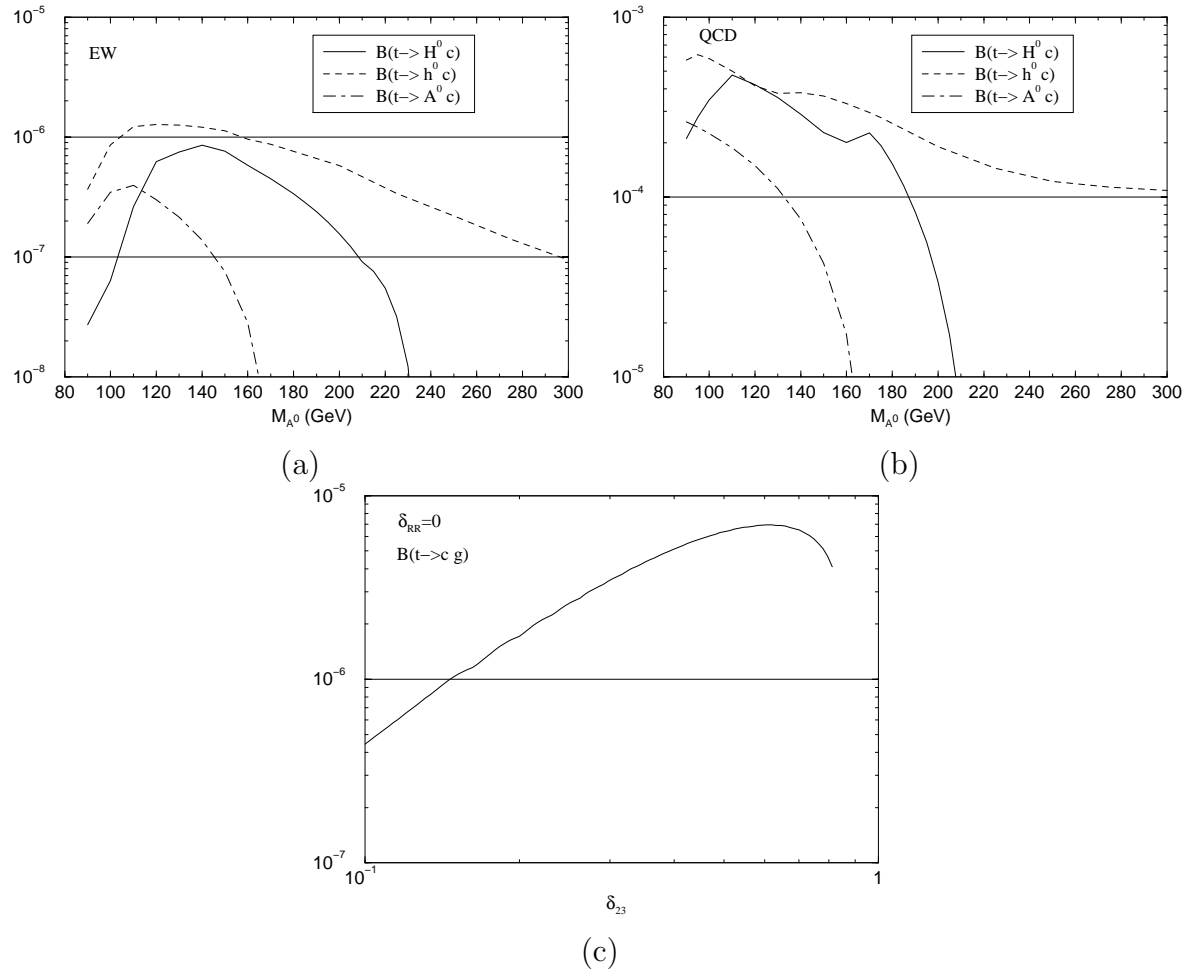


Figure 3: **(a)** Maximum value of $B(t \rightarrow ch)$, obtained by taking into account only the SUSY-EW contributions, as a function of M_{A^0} ; **(b)** as in (a) but taking into account only the SUSY-QCD contributions; and **(c)** maximum value of $B(t \rightarrow cg)$ as a function of the intergenerational mixing parameter δ_{23} in the LH sector. In all cases the scanning for the rest of parameters of the MSSM has been performed within the phenomenologically allowed region.

magnitude larger, and they exhibit a slow decoupling as a function of the gluino mass, so even for gluinos as heavy as $m_{\tilde{g}} \simeq 500$ GeV the ratio $B(t \rightarrow ch^0)$ can reach the level of 10^{-5} . This large value is due to the strong nature of the gluino-mediated interactions, but not less to the fact that present bounds on δ_{23} are rather poor. Also the various decays are sensitive to both: the higgsino mass parameter μ and the soft-SUSY-breaking trilinear coupling A_t .

In Figs. 3a and b we present the result of maximizing the ratio (6) for the SUSY-EW and SUSY-QCD contributions respectively [27]. These plots have been obtained by performing a full scan of the MSSM parameter space, in the phenomenologically allowed region, and for SUSY parameters below 1 TeV. Needless to say, not all of the maxima can be simultaneously attained as they are obtained for different values of the parameters. Perhaps the most noticeable result is that the decay into the lightest MSSM Higgs boson ($t \rightarrow ch^0$) is the one that can be maximally enhanced, reaching values of order $B(t \rightarrow$

$ch^0) \sim 10^{-4}$ that stay fairly stable all over the parameter space, and in particular for almost all the range of allowed Higgs boson masses in the MSSM.

For the sake of comparison, in Fig. 3 we show the maximized ratio for the competing decay $t \rightarrow cg$ as a function of the intergenerational mixing parameter between the second and the third generation, δ_{23} (5). We see that it never really reaches the critical value 10^{-5} , which can be considered as the visible threshold for the next generation of high luminosity colliders. To assess the discovery reach of the FCNC top quark decays for these future accelerators we take as a guide the estimations that have been made for gauge boson final states [34]. Assuming that all the FCNC decays $t \rightarrow cX$ ($X = V, h$) can be treated similarly, we roughly estimate the following sensitivities for 100 fb^{-1} of integrated luminosity:

$$\textbf{LHC} : B \gtrsim 5 \times 10^{-5} ; \textbf{LC} : B \gtrsim 5 \times 10^{-4} ; \textbf{TEV33} : B \gtrsim 5 \times 10^{-3} . \quad (7)$$

Although the LHC seems to be the most sensitive machine to this kind of physics (due to its highest luminosity) the LC is also very competitive due to the cleanliness of its environment which should allow a much more efficient isolation of the rare events. The upgraded Tevatron, unfortunately, looks not so promising in this respect.

To better assess the realistic possibilities for detecting the most serious FCNC top quark decay candidates, $t \rightarrow ch$ and $t \rightarrow cg$, we remark that around the loci of maximal rates in parameter space the following situation is achieved

$$5 \times 10^{-6} \lesssim B(t \rightarrow cg)_{\max} < B(t \rightarrow ch^0)_{\max} \lesssim 5 \times 10^{-4} . \quad (8)$$

In both types of decays the dominant effects come from SUSY-QCD. However, it should not be undervalued the fact that the maximum electroweak rates for $t \rightarrow ch$ can reach the 10^{-6} level. Last but not least, we stress once again that the largest FCNC rate both from SUSY-QCD and SUSY-EW is precisely that of the lightest CP-even state ($t \rightarrow ch^0$), which is the only Higgs channel that is phase-space available across the whole MSSM parameter space.

2.4 Two-body decays into R -odd particles

In principle there exist three possible two-body decays of the top quark into R -odd particles: $t \rightarrow \tilde{b}\chi^+$, $t \rightarrow \tilde{t}\tilde{g}$ and $t \rightarrow \tilde{t}\chi^0$. These decays were reviewed in [35]. From the latest combined analysis of the four LEP experiments a lower bound on the squark and chargino masses between 80 GeV and 90 GeV is obtained [36]. The exact bound depends on the assumptions of the analysis. The chargino channel is then highly disfavoured, and might be already closed at the end of the present LEP run. The light gluino window ($m_{\tilde{g}} \lesssim 5 \text{ GeV}$) still exists, but its importance is everyday more marginal [37]. Otherwise the direct limits from the Tevatron $m_{\tilde{g}} \gtrsim 200 \text{ GeV}$ [38] apply, and the gluino decay channel is completely ruled out. So we are left with the neutralino decay channel as the most interesting decay. Note that light top-squarks are a natural feature in the MSSM due to the large top quark Yukawa coupling, and the presence of large mixing in the stop sector. A light top-squark (with small $\tan \beta$) also leads to an enhancement of R_b , pushing it closer to the measured value [39]. Under the conditions of light stop and low $\tan \beta$ the

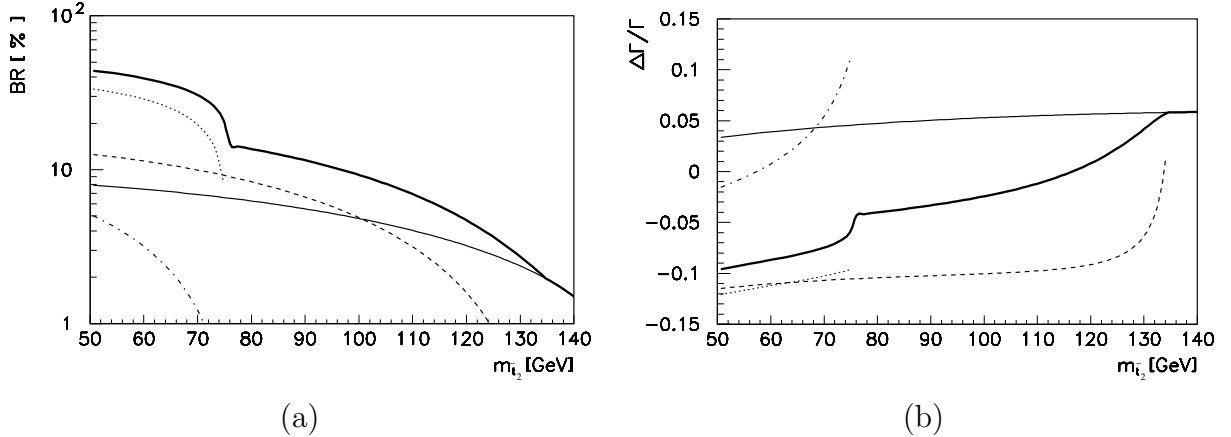


Figure 4: **(a)** The tree-level prediction for $\text{BR}(t \rightarrow \tilde{t}\chi_\alpha^0)$ as a function of the lightest stop mass. **(b)** The one-loop SUSY-QCD corrections to $\Gamma(t \rightarrow \tilde{t}\chi_\alpha^0)$. $M_2 = -\mu = 50$ GeV, $\tan\beta = 1.6$ $m_t = 180$ GeV. The thin, solid, dashed and dash-dotted lines correspond respectively to $\alpha = 1 - 4$, the thick solid line corresponds to the sum over all neutralinos. $m_{\tilde{g}} (\simeq 180$ GeV) is fixed from GUT relations. From Ref. [40].

branching ratio for the top quark decay into a neutralino and a stop can be at the 20% to 30% level. The strong sector one-loop radiative corrections to this partial decay width have been computed in [40, 41]. A key feature of the radiative corrections in which R -odd and R -even particles are both involved in external legs is that it is no longer possible to separate between standard and SUSY corrections, since neither of these subsets is finite by itself, so gluon and gluino loop contributions must be added up in order to obtain a finite result. As a consequence of that there appear terms which present non-decoupling, namely corrections proportional to $\alpha_s \log(m_{\tilde{g}}/m_{\tilde{t}_a})$.

The on-shell renormalization procedure must again deal with non-standard counterterms. In this case a counterterm for the stop mixing angle, $\delta\theta_t$, is necessary, even in the case of vanishing angle; this can be fixed by the condition that $\delta\theta_t$ cancels the one-loop mixing two-point function between the two stops at $m_{\tilde{t}_2}$ [40].

In Fig. 4a we see the tree-level prediction for the various branching ratios $B(t \rightarrow \tilde{t}\chi_\alpha^0)$ as a function of the lightest stop mass. We see that large values of this branching ratio can be obtained. In Fig. 4b the radiative QCD corrections to each of the decays are plotted. Their absolute value lies in the range 2 – 12%, for the small values of the gluino mass ($m_{\tilde{g}} \simeq 180$ GeV) used in this figure. For larger gluino masses the corrections are negative, and in the range $m_{\tilde{g}} = 1 - 5$ TeV they grow from –12% to –22% [40].

2.5 Three-particle decays

In order to have a consistent description of the top quark decay width at the order $G_F\alpha$ it is necessary to account for the three-body decays of the top quark as well. In Ref. [3] all the possible three-body decays of the top quark were investigated.⁶ The aim in that work was to concentrate the analysis in regions of the parameter space in which

⁶See also Ref. [42] for a recent analysis of some of these modes, including R -parity violating decays.

the corresponding two-body decays were phase-space closed. With the latest bounds on SUSY particle masses [36] some of these decays turn out to be phase-space closed. Here we briefly review those that still are kinematically allowed.

$t \rightarrow b\tau^+\nu_\tau$: In the MSSM there exists, in addition to the gauge boson mediated channel, also the charged Higgs boson one. Of course, if the charged Higgs is lighter than the top quark then it would proceed through the two-body decay $t \rightarrow H^+b$ analyzed in section 2.2. But if the charged Higgs is heavier than the top quark, then the additional contribution to the $\tau^+\nu_\tau$ final state from the H^+ mediated diagram is in the range of 1-3% for $M_{H^\pm} < 200$ GeV and large $\tan\beta > 40$; $t \rightarrow bW^+h^0$: Its decay width can only reach at most $\Gamma/\Gamma_{SM}^0 \lesssim 3 \times 10^{-4}$.

Next we just quote the maximum branching ratios for some decays into R -odd particles. $t \rightarrow b\chi^0\chi^+$: $\Gamma/\Gamma_{SM}^0 \lesssim 0.006$; $t \rightarrow \tilde{b}\tau^+\tilde{\nu}_\tau$: $\Gamma/\Gamma_{SM}^0 \lesssim 1\%$; $t \rightarrow b\tilde{g}\chi^+$: We remark that this decay could only be possible in the light gluino scenario, but even in this case $\Gamma/\Gamma_{SM}^0 \lesssim 4\%$. Let us comment now a bit on the decay $t \rightarrow \tilde{b}\tilde{\tau}\tilde{\nu}_\tau$. This is an interesting process since, although it contains two R -odd particles in the final state, both of them are sleptons, which therefore evade the limits from hadron colliders, and being from the third generation they are expected to be light. Two Feynman diagrams contribute to the amplitude of this process, one of them involves the exchange of a charged Higgs particle. Part of the couplings between H^+ and the $\tilde{\tau} - \tilde{\nu}_\tau$ state involve the combination $A_\tau \tan\beta + \mu$, which can naturally reach large values. It turns out that if the decay channel $H^+ \rightarrow \tilde{\tau}\tilde{\nu}_\tau$ is closed (i.e. $M_{H^\pm} < m_{\tilde{\tau}} + m_{\tilde{\nu}_\tau}$) the value of this partial decay width is enhanced. The maximum value of the partial decay width is obtained for M_{H^\pm} slightly below the sum of the slepton masses. With this condition, together with large $\tan\beta \gtrsim 40$, and $|\mu| \gtrsim 100$ GeV we find that the values for the corresponding branching ratio can easily be of 50% [3]. Of course, this kind of precise alignment may be not the most natural expectation in the MSSM, but even if the parameters are not “optimized” for a maximum branching ratio, there exist regions (in the large $\tan\beta$ scenario) where it can be relevant, say above the 10% level. One of the possible signals for this decay channel includes a τ^- , i.e. a “wrong sign” lepton, which could help in identifying this decay chain. See Ref. [3] for a complete compilation of possible distinctive signals.

3 Top-quark pair production in $e^+e^- \rightarrow t\bar{t}$

Besides the possibility of direct production of SUSY particles at sufficiently high energies, accurate investigations of the production of standard fermion pairs in e^+e^- annihilation offers the indirect search for virtual SUSY particles through quantum effects in terms of loop corrections. In particular the top quark, owing to its large mass, is an ideal probe of all those virtual effects that grow with the fermion mass scale, such as Yukawa interactions and CP violation. The MSSM with complex parameters induces CP-violating observables already at the one-loop level; they are described below after a brief discussion of the generic supersymmetric loop contributions to the CP-conserving cross section for $t\bar{t}$ production.

3.1 Loop effects in the CP-conserving MSSM

The process of $t\bar{t}$ production is in lowest order described by photon and Z -boson exchange. The cross section can be written as follows

$$\sigma^{(0)}(e^+e^- \rightarrow t\bar{t}) = \frac{\beta}{4\pi s} \left[\frac{3-\beta^2}{2} \sigma_V(s) + \beta^2 \sigma_A(s) \right] \quad (9)$$

with

$$s = (p_{e^-} + p_{e^+})^2, \quad \beta = \sqrt{1 - \frac{4m_t^2}{s}}, \quad (10)$$

and

$$\begin{aligned} \sigma_V &= Q_e^2 Q_t^2 e(s)^4 + 2v_e v_t Q_e Q_t e(s)^2 \chi(s) + (v_e^2 + a_e^2) v_t^2 \chi(s)^2, \\ \sigma_A &= (v_e^2 + a_e^2) a_t^2 \chi(s)^2. \end{aligned} \quad (11)$$

This expression is an effective Born approximation, which incorporates the effective (running) electromagnetic charge containing the photon vacuum polarization (real part)

$$e(s)^2 = \frac{4\pi\alpha}{1 - \Delta\alpha(s)}, \quad (12)$$

the Z propagator, together with the overall normalization factor of the neutral-current couplings in terms of the Fermi constant G_μ ,

$$\chi(s) = (G_\mu M_Z^2 \sqrt{2})^2 \frac{s}{s - M_Z^2}, \quad (13)$$

and the vector and axial-vector coupling constants for $f = e, t$,

$$v_f = I_3^f - 2Q_f \sin^2 \theta_W, \quad a_f = I_3^f. \quad (14)$$

The complete electroweak one-loop corrections were calculated for the case of the Standard Model [43, 44], including also the hard-photon QED corrections [45]. In a more recent study [46], a complete one-loop calculation was performed for the MSSM electroweak corrections and the non-standard part of the QCD corrections (SUSY-QCD corrections) to $e^+e^- \rightarrow t\bar{t}$. The virtual Higgs contributions have also been derived in a general 2-Higgs-doublet model [47]. For a large mass of the A^0 boson in the MSSM Higgs sector, the heavy particles H^0, A^0, H^\pm decouple and the light h^0 scalar behaves like the standard Higgs boson. In this so-called decoupling limit, the only non-standard virtual SUSY effects arise from the genuine supersymmetric particles.

The one-loop contribution to the S -matrix element contains the γ and Z self-energies, the γ and Z vertex corrections together with the external wave function renormalization, and the box diagrams. Since Higgs-boson couplings to the initial state e^+, e^- are negligible, we only have to consider the standard box graphs with Z and W^\pm exchange and the SUSY box graphs with neutralino and chargino exchange.

The complete set of vertex corrections comprises the QED corrections with virtual photons and the QCD corrections with virtual gluons. They need real photon and gluon

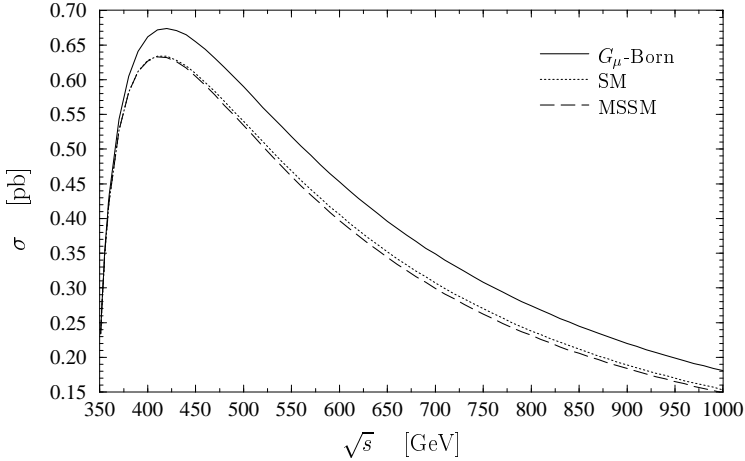


Figure 5: The cross section for $e^+e^- \rightarrow t\bar{t}$, as a function of the energy. $\sqrt{s} = 500$ GeV, $M_A = 500$ GeV, $m_{\tilde{t}_1} = 100$ GeV, $m_{\chi_1^\pm} = 100$ GeV, $A = 500$ GeV, $\mu = -150$ GeV, $\tan \beta = 40$.

bremsstrahlung for a infrared-finite result. The gauge-invariant subclasses of “standard QED” and “standard QCD” corrections are identical to those in the Standard Model and are available in the literature [43, 45, 48]. In the meantime, also a combined treatment of the QCD and the electroweak radiative corrections in the Standard Model has been proposed [49] in order to account for the dominant terms from both sources. In our context, we are interested in deviations from the Standard Model induced by non-standard virtual particles. We therefore concentrate our discussion on the set of model-dependent and IR-finite virtual corrections, without the diagrams involving virtual photons and gluons. The supersymmetric part of the QCD corrections, arising from virtual gluinos, is included as part of the final-state vertex correction.

The effect of these IR-finite loop-corrections is illustrated in Figure 5, where the energy dependence of lowest-order cross section (9) is shown together with the Standard Model (SM) and the MSSM one-loop prediction. The differences between the SM and the MSSM depend on the values of the SUSY-breaking parameters and the Higgsino mass parameter μ . In case of a direct detection of SUSY particles, these parameters can, at least partially, be measured and the top production cross section can provide an independent test of the MSSM. In a first phase of a Linear Collider operation, the mass of eventually light SUSY particles, such as a scalar top \tilde{t}_1 or a chargino χ_1^\pm may be determined sufficiently well, while the heavier particles may appear as less accessible. A precise measurement of the $t\bar{t}$ cross section is therefore useful to probe the heavier part of the model through the quantum contributions. To make this more quantitative, we assume a scenario with a relatively light stop and chargino, and analyze the dependence of the loop-contributions on the residual parameters of the MSSM, which determine the heavier part of the mass spectrum. In order to exhibit the deviations from the SM, we introduce the quantity

$$\Delta = \frac{\sigma^{\text{MSSM}}(s) - \sigma^{\text{SM}}(s)}{\sigma^{(0)}(s)}, \quad (15)$$

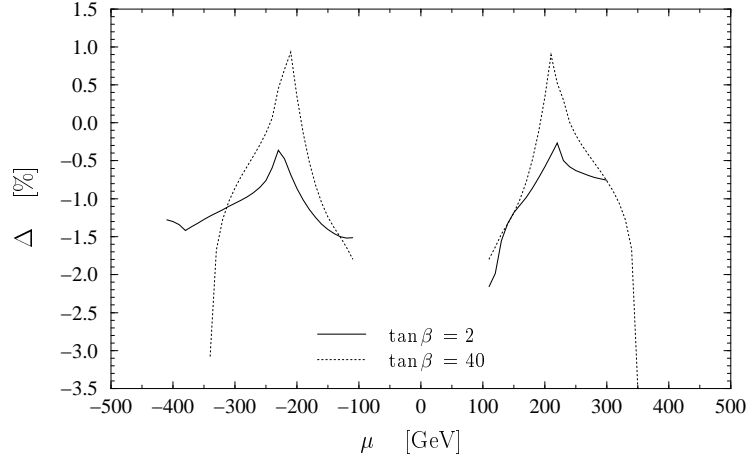


Figure 6: Difference between MSSM and SM, relative to the Born cross section, for a light stop and chargino. $\sqrt{s} = 500$ GeV, $M_A = 500$ GeV, $m_{\tilde{t}_1} = 100$ GeV, $m_{\chi_1^\pm} = 100$ GeV, $A = 500$ GeV.

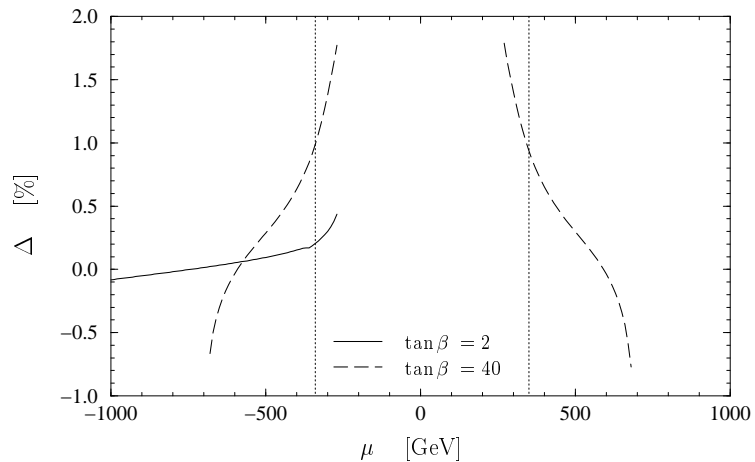


Figure 7: Difference between MSSM and SM, relative to the Born cross section for heavy SUSY particles. $\sqrt{s} = 500$ GeV, $M_A = 500$ GeV, $m_{\tilde{t}_1} = 260$ GeV, $m_{\chi_1^\pm} = 260$ GeV, $A = 500$ GeV. The range consistent with the constraints is between the vertical lines for the large $\tan \beta$ case only; the solid line is not constrained.

which gives the difference between the models normalized to the Born cross section (9). The results are displayed in Figure 6. For simplicity, we have assumed a common mass scale M_S and a common A parameter for the diagonal and non-diagonal entries in the sfermion mass-square matrices of all generations (as well as for L and R chiralities). The free parameters in Figure 6 are varied in accordance with a set of constraints which ensure consistency with the present electroweak precision data and bounds from direct Higgs searches. The effects are in the per-cent range, and show quite some sensitivity to the model parameters. Large values for $\tan\beta$ induce bigger loop effects, owing to the enhanced b quark/squark Yukawa couplings.

As another possible scenario, we consider the situation that SUSY particles are not directly detected at a 500 GeV collider. The corresponding virtual SUSY effects, compatible with these bounds and with the constraints from the electroweak precision data, are shown in Figure 7. At least for the large- $\tan\beta$ regime the loop contributions are at the level of 1–2 per cent.

3.2 CP violation in the MSSM

3.2.1 The MSSM with complex couplings

The following parameters of the MSSM with preserved R -parity may take complex values: the Yukawa couplings, the μ parameter and the soft-breaking parameters m_{12}^2 (in the Higgs potential), M_1 , M_2 , M_3 (gaugino mass terms) and A (trilinear terms). But not all of the complex phases introduced are physical since several of them can be absorbed by redefinitions of the fields.

We assume the GUT relation between the M_i , so they have one common phase. The remaining phases are chosen to be those of μ , the A parameters and, for three generations, one phase for all the Yukawa couplings, the δ_{CKM} . Analogous to the Standard Model case, the Yukawa couplings can be changed by redefinitions of the quark superfields in such a way that there remains only one phase for three generations.

Furthermore, the $\mathcal{L}_{\text{MSSM}}$ is invariant under two U(1) transformations, the Peccei-Quinn symmetry and the R -symmetry, that do not only transform the fields but also the parameters of the MSSM [50]. With them one can easily show [51] that the physical predictions only depend on the absolute values of the parameters and the phases

$$\phi_A \equiv \arg(AM_i^*), \quad \phi_B \equiv \arg(\mu Am_{12}^{2*}). \quad (16)$$

It is then possible to choose a set where only the μ and the A parameters are complex. We take $\varphi_\mu = \arg(\mu)$ and the phase of A is traded for the phase φ_f of the off-diagonal term in the corresponding sfermion mixing matrix: $m_{LR}^f \equiv A_f - \mu^* \{\cot, \tan\} \beta$, for {up, down}-type fermions, respectively. Relaxing universality for the soft-breaking terms, every A_f has a different phase.

In comparison with the MSSM with real couplings, the new physical phases affect the mass spectrum of charginos and neutralinos, modify the tree level couplings and notably produce CP-violating effects at the one-loop level that we analyze in the following.

3.2.2 Electric dipole form factors

The most general Lorentz structure for the vertex Vff in the momentum space is

$$\begin{aligned}\Gamma_\mu^{Vff} = & i \left[\gamma_\mu (f_V - f_A \gamma_5) + (q - \bar{q})_\mu (f_M + i f_E \gamma_5) + p_\mu (i f_S + f_P \gamma_5) \right. \\ & \left. + (q - \bar{q})^\nu \sigma_{\mu\nu} (f_{TS} + i f_{TP} \gamma_5) + p^\nu \sigma_{\mu\nu} (i f_{TM} + f_{TE} \gamma_5) \right],\end{aligned}\quad (17)$$

where q and \bar{q} are the outgoing momenta of the fermions and $p = (q + \bar{q})$ is the total incoming momentum of the neutral vector boson V . The form factors f_i are functions of kinematical invariants and can be complex in general. Their real parts account for dispersive effects (CPT-even) whereas their imaginary parts are related to absorptive contributions. For on-shell fermions, making use of the Gordon identities, one can eliminate f_{TM} , f_{TE} , f_{TS} and f_{TP} . The number of relevant form factors can be further reduced when V is on shell, since then the condition $p_\mu \epsilon^\mu = 0$ cancels the contributions coming from f_S and f_P . The form factors f_V and f_A are connected to the chirality conserving, CP-even sector. The anomalous magnetic and electric dipole form factors are defined, respectively, by

$$\text{AMDFF} \equiv a_f^V(s) \equiv -2m_f f_M(s), \quad (18)$$

$$\text{EDFF} \equiv d_f^V(s) \equiv e f_E(s). \quad (19)$$

They are related to chirality-flipping operators of dimension larger than four. In a renormalizable theory they can receive contributions exclusively by quantum corrections. Unlike the MDFFs, the EDFFs are connected to the CP-odd sector and therefore constitute a source of CP violation. The *electromagnetic* and *weak dipole moments* are physical and gauge invariant quantities corresponding to the values of the dipole form factors at $s = (q + \bar{q})^2 = M_V^2$ for $V = \gamma, Z$, respectively.

All the possible one-loop contributions to the $a_f^V(s)$ and $d_f^V(s)$ form factors can be classified in terms of the six classes of triangle diagrams. The vertices involved are labeled by generic couplings according to a general interaction Lagrangian. Every class of diagrams has been calculated analytically and expressed, in the 't Hooft-Feynman gauge, in terms of masses, generic (complex) couplings and one-loop 3-point integrals in Refs. [52, 53].

We concentrate here on the CP-violating electric dipoles of the top quark. Unlike the SM, where the EDFFs arise first at three loops [54], in the MSSM they receive contributions already at the one-loop level [51, 53, 55]. On the other hand, since the top quark is too heavy to be pair-produced by Z decays, and has a too short life to study its electromagnetic static properties, the electric $d_t^\gamma(s)$ and weak-electric $d_t^Z(s)$ form factors, $s > 4m_t^2$, are *not physical*. In fact, they do not contribute alone to CP-violating observables, as it will be shown in next Section. Nevertheless they happen to be gauge invariant quantities at one loop.

The size of the electric dipole form factors of the top quark is illustrated in Fig. 8 where the different contributions from charginos, neutralinos and gluinos are also displayed. Neutralinos and gluinos appear with stops in the loops, and charginos with sbottoms. The Higgs sector does not play any role. The results depend on a number of MSSM parameters: $\tan \beta$, M_2 , $|\mu|$, m_{LR}^t , m_{LR}^b and $m_{\tilde{q}}$ (the common squark mass parameter); and

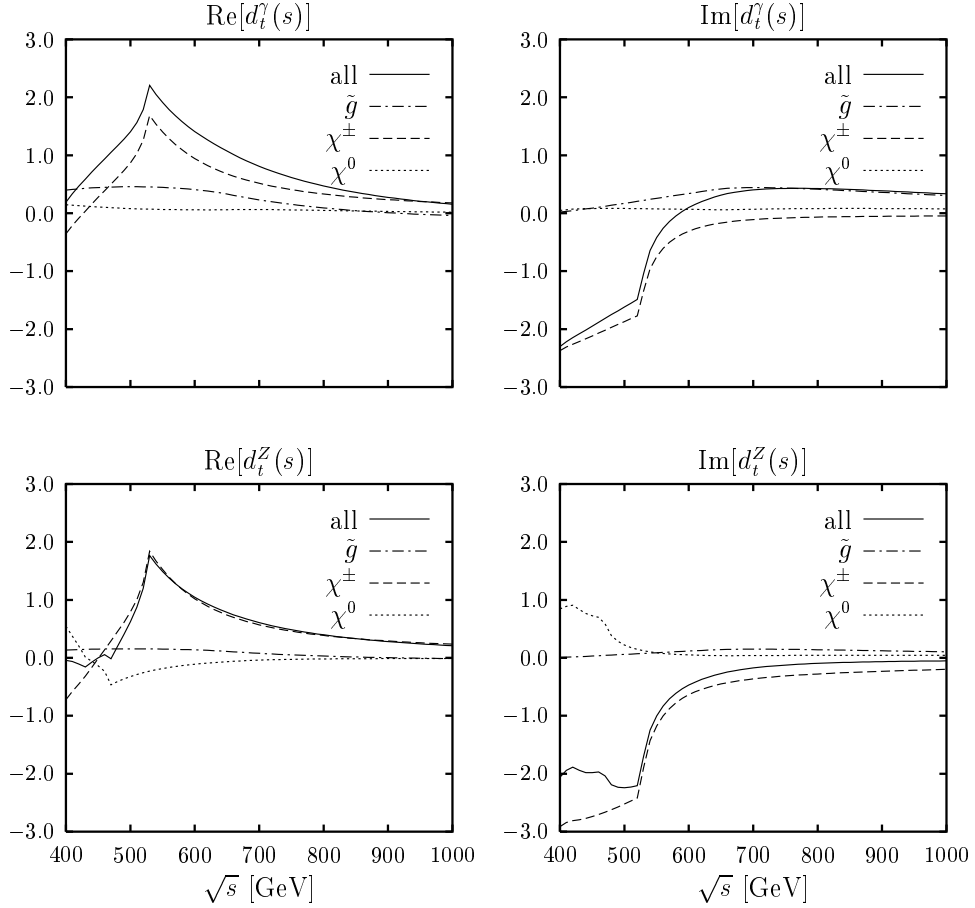


Figure 8: The contributions to the t (W)EDFF/ $10^{-3}\mu_t$ for Set #1 of MSSM parameters (20).

three physical CP-violating phases, φ_μ , $\varphi_{\tilde{t}}$ and $\varphi_{\tilde{b}}$. They are expressed in t magnetons $\mu_t \equiv e/2m_t = 5.64 \times 10^{-17} e$ cm. The values shown in the plots are for the set of inputs:

$$\begin{aligned}
 \tan \beta &= 1.6 \\
 M_2 = |\mu| = m_{\tilde{q}} &= |m_{LR}^t| = |m_{LR}^b| = 200 \text{ GeV} \\
 \text{Reference Set \#1 : } \varphi_\mu &= -\varphi_{\tilde{t}} = -\varphi_{\tilde{b}} = \pi/2.
 \end{aligned} \tag{20}$$

This set of parameters is plausible and enhances the electric dipole form factors in the vicinity of $\sqrt{s} = 500$ GeV, due to threshold effects (spikes in Fig. 8). The phases are chosen maximal and with such a sign that the typically larger components (charginos and gluinos) add up constructively. The low $\tan \beta$ scenario has been chosen because both chargino and gluino contributions are then larger. Of course, the electric dipoles vanish for zero phases. Due to the decoupling of the supersymmetric sector, the dipoles tend to vanish for increasing values of the mass parameters. A detailed study can be found in [51].

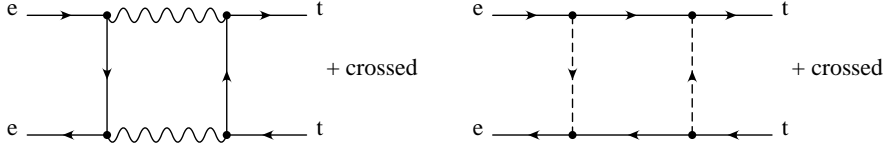


Figure 9: Relevant generic box graphs for the MSSM at one loop. The first class involves only SM particles and does not contribute to CP violation.

3.2.3 CP-odd observables

Not only vertex- but also box-diagrams correct the tree level process to one loop. Accordingly, any CP-odd observable will depend on the CP-violating effects due to vertex corrections included in the electric and weak-electric dipole form factors as well as on CP-violating box contributions. In the former there appear either sneutrinos, neutralinos and stops or selectrons, charginos and sbottoms.

To probe CP violation, consider the pair-production of polarized t quarks $e^+(\mathbf{p}_+) + e^-(\mathbf{p}_-) \rightarrow t(\mathbf{k}_+, \mathbf{s}_1) + \bar{t}(\mathbf{k}_-, \mathbf{s}_2)$. The decay channels labeled by a and c act as spin analyzers in $t + \bar{t} \rightarrow a(\mathbf{q}_+) + \bar{c}(\mathbf{q}_-) + X$. The momenta and polarization vectors in the overall c.m.s. transform under CP and CPT as follows:⁷

$$\begin{array}{ll} \text{CP : } & \mathbf{p}_\pm \rightarrow -\mathbf{p}_\mp = \mathbf{p}_\pm \\ & \mathbf{k}_\pm \rightarrow -\mathbf{k}_\mp = \mathbf{k}_\pm \\ & \mathbf{q}_\pm \rightarrow -\mathbf{q}_\mp \\ & \mathbf{s}_1 \leftrightarrow \mathbf{s}_2 \\ \text{CPT : } & \mathbf{p}_\pm \rightarrow \mathbf{p}_\mp = -\mathbf{p}_\pm \\ & \mathbf{k}_\pm \rightarrow \mathbf{k}_\mp = -\mathbf{k}_\pm \\ & \mathbf{q}_\pm \rightarrow \mathbf{q}_\mp \\ & \mathbf{s}_1 \leftrightarrow -\mathbf{s}_2 \end{array} \quad (21)$$

From the unit momentum of one of the t quarks in the c.m.s. (say $\hat{\mathbf{k}}_+$) and their polarizations ($\mathbf{s}_1, \mathbf{s}_2$) a basis of linearly independent CP-odd *spin observables* can be constructed [56]. The spin observables are related to more realistic (directly measurable) *momentum observables* based on the momenta of the top decay products [57]. The polarizations can be analyzed through the angular correlation of the weak decay products, both in the nonleptonic and in the semileptonic channels:

$$t(\mathbf{k}_+) \rightarrow b(\mathbf{q}_b) X_{\text{had}}(\mathbf{q}_x), \quad (22)$$

$$t(\mathbf{k}_+) \rightarrow b(\mathbf{q}_b) \ell^+(\mathbf{q}_+) \nu_\ell \quad (\ell = e, \mu, \tau) \quad (23)$$

and the charged conjugated ones.

3.2.4 Spin observables

A list of CP-odd spin observables classified according to their CPT properties is shown in Table 1. Their expectation values as a function of s and the scattering angle of the t quark in the overall c.m. frame are given by

$$\langle \mathcal{O} \rangle_{\mathbf{ab}} = \frac{1}{2d\sigma} \left[\sum_{\mathbf{s}_1^*, \mathbf{s}_2^* = \pm \mathbf{a}, \pm \mathbf{b}} + \sum_{\mathbf{s}_1^*, \mathbf{s}_2^* = \pm \mathbf{b}, \pm \mathbf{a}} \right] d\sigma(\mathbf{s}_1^*, \mathbf{s}_2^*) \mathcal{O}, \quad (24)$$

⁷T means reflection of spins and momenta.

i	CPT	\mathcal{O}_i	a	b	Set #1		Set #2	
1	even	$(\mathbf{s}_1^* - \mathbf{s}_2^*)_y$	T \uparrow	T \downarrow	1.216	-0.231	0.207	-1.394
2	even	$(\mathbf{s}_1^* \times \mathbf{s}_2^*)_x$	T \uparrow	L \uparrow	-0.755	-0.489	-0.053	0.318
3	even	$(\mathbf{s}_1^* \times \mathbf{s}_2^*)_z$	N \uparrow	T \uparrow	1.184	0.625	0.090	-0.598
4	odd	$(\mathbf{s}_1^* - \mathbf{s}_2^*)_x$	N \uparrow	N \downarrow	-1.230	-1.421	-1.888	-2.217
5	odd	$(\mathbf{s}_1^* - \mathbf{s}_2^*)_z$	L \uparrow	L \downarrow	2.550	2.739	3.823	4.216
6	odd	$(\mathbf{s}_1^* \times \mathbf{s}_2^*)_y$	L \uparrow	T \downarrow	-1.683	-1.751	-2.050	-2.216

Table 1: Ratio $r \equiv \langle \mathcal{O} \rangle / \sqrt{\langle \mathcal{O}^2 \rangle}$ [in 10^{-3} units] of the integrated spin observables at $\sqrt{s} = 500$ GeV for the Set #1 (20) and Set #2 (26) of MSSM parameters. The left column excludes the box corrections and the right one comes from the complete one-loop cross section for $e^+e^- \rightarrow t\bar{t}$.

$$d\sigma = \sum_{\pm \mathbf{s}_1^*, \pm \mathbf{s}_2^*} d\sigma(\mathbf{s}_1^*, \mathbf{s}_2^*). \quad (25)$$

They are displayed in Fig. 10, for two sets of MSSM parameters, Set #1 of (20) and Set #2 with same moduli but different phases:

$$\text{Reference Set \#2 :} \quad \varphi_\mu = \varphi_{\bar{t}} = \varphi_{\bar{b}} = \pi/2. \quad (26)$$

The directions of polarization of t and \bar{t} (**a** and **b**) are taken normal to the scattering plane (N), transversal (T) or longitudinal (L). They are taken either parallel (\uparrow) or antiparallel (\downarrow) to the axes defined by $\hat{z} = \mathbf{k}_+$, $\hat{y} = \mathbf{k}_+ \times \mathbf{p}_+ / |\mathbf{k}_+ \times \mathbf{p}_+|$ and $\hat{x} = \hat{y} \times \hat{z}$. The spin vectors \mathbf{s}_1^* , \mathbf{s}_2^* are defined in the t , \bar{t} rest frames, respectively. The statistical significance (number of standard deviations) of the CP-violation signal is given by

$$N_{SD} = |r| \sqrt{N}, \quad r \equiv \langle \mathcal{O} \rangle / \sqrt{\langle \mathcal{O}^2 \rangle} \quad (27)$$

where N is the number of observed events.

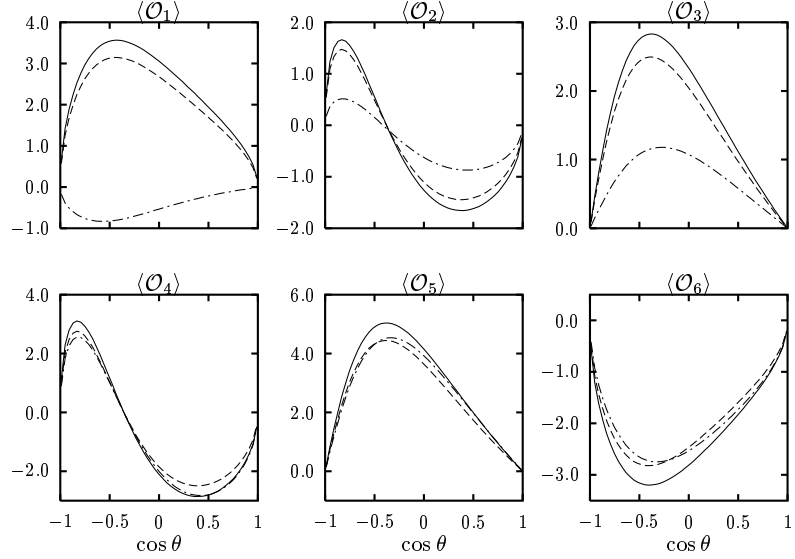
We compare the result when only the self energies and vertex corrections are included (left column) with the complete one-loop calculation (right column). The shape of the observables as a function of the t polar angle is also quite different when the CP violating box contributions are taken into account (Fig. 10). This illustrates that the *dipole form factors* of the t quark are *not sufficient to parameterize observable CP-violating effects* and the predictions can be wrong by far.

3.2.5 Momentum observables

Consider now the decay channels labeled by a and c acting as spin analyzers in $t + \bar{t} \rightarrow a(\mathbf{q}_+) + \bar{c}(\mathbf{q}_-) + X$. We ignore here possible CP violation in the top-quark decays, that may occur due to supersymmetric one-loop corrections [58]. The expectation value of a realistic CP-odd observable is given by the average over the phase space of the final state particles,

$$\langle \mathcal{O} \rangle_{ac} = \frac{1}{2} [\langle \mathcal{O} \rangle_{a\bar{c}} + \langle \mathcal{O} \rangle_{c\bar{a}}] = \frac{1}{2\sigma_{ac}} \int [d\sigma_{a\bar{c}} + d\sigma_{c\bar{a}}] \mathcal{O}, \quad (28)$$

Reference Set #1



Reference Set #2

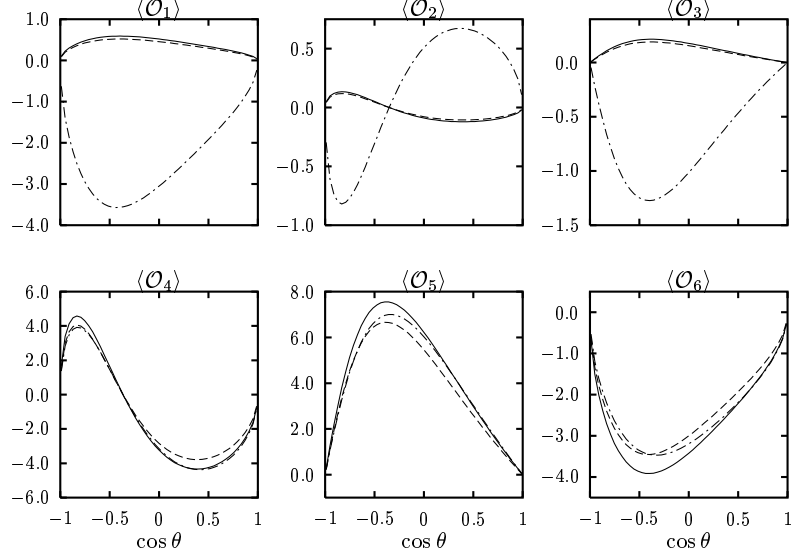


Figure 10: Expectation value of the spin observables [in 10^{-3} units] for the two reference sets of MSSM parameters, assuming for the cross section: (i) tree level plus contribution from (W)EDFFs only (solid line); (ii) one loop including all the vertex corrections and the self-energies (dashed line); (iii) complete one loop (dot-dashed line).

where both the process $(a\bar{c})$ and its CP conjugate $(c\bar{a})$ are included and

$$\sigma_{ac} = \int d\sigma_{a\bar{c}} = \int d\sigma_{c\bar{a}}, \quad (29)$$

The differential cross section for t -pair production and decay is evaluated for every channel using the narrow width approximation. As $m_t > M_W + m_b$, the t quark decays proceed predominantly through Wb . Within the SM the angular distribution of the charged lepton is a much better spin analyzer of the t quark than that of the b quark or the W boson arising from semileptonic or nonleptonic t decays [59]. The dimensionless observables are easier to measure, for instance the scalar CP-odd observables [56]:

$$\hat{A}_1 \equiv \hat{\mathbf{p}}_+ \cdot \frac{\hat{\mathbf{q}}_+ \times \hat{\mathbf{q}}_-}{|\hat{\mathbf{q}}_+ \times \hat{\mathbf{q}}_-|} \quad [\text{CPT-even}] \quad (30)$$

$$\hat{A}_2 \equiv \hat{\mathbf{p}}_+ \cdot (\hat{\mathbf{q}}_+ + \hat{\mathbf{q}}_-) \quad [\text{CPT-odd}] \quad (31)$$

or the CP-odd traceless tensors [56]:

$$\hat{T}_{ij} \equiv (\hat{\mathbf{q}}_+ - \hat{\mathbf{q}}_-)_i \frac{(\hat{\mathbf{q}}_+ \times \hat{\mathbf{q}}_-)_j}{|\hat{\mathbf{q}}_+ \times \hat{\mathbf{q}}_-|} + (i \leftrightarrow j) \quad [\text{CPT-even}] \quad (32)$$

$$\hat{Q}_{ij} \equiv (\hat{\mathbf{q}}_+ + \hat{\mathbf{q}}_-)_i (\hat{\mathbf{q}}_+ - \hat{\mathbf{q}}_-)_j + (i \leftrightarrow j) \quad [\text{CPT-odd}] \quad (33)$$

The reconstruction of the t frame is not necessary for the momentum observables. The observables \hat{A}_2 and \hat{Q}_{ij} do not involve angular correlations as they could be measured considering separate samples of events in the reactions $e^+e^- \rightarrow aX$ and $e^+e^- \rightarrow \bar{a}X$. Nevertheless it is convenient to treat them in an event-by-event basis [56].

In Table 2 the ratio r is shown for three different decay channels at $\sqrt{s} = 500$ GeV. The CP-odd observables involve the momenta of the decay products analyzing t and \bar{t} polarizations in the laboratory frame. The leptonic decay channels are the best t spin analyzers but the number of leptonic events is also smaller. The Reference Set #2 has been chosen. As expected, the dipole contributions (left columns) to the CPT even observables are very small for this choice of MSSM parameters but the *actual* expectation values (right columns) are larger.

CPT	\mathcal{O}	$b - b$		$\ell - b$		$\ell - \ell$	
even	\hat{A}_1	-0.036	0.242	0.030	-0.202	0.068	-0.467
odd	\hat{A}_2	0.270	0.304	-0.180	-0.204	-0.501	-0.812
even	\hat{T}_{33}	-0.006	0.042	0.021	-0.140	-0.037	0.248
odd	\hat{Q}_{33}	0.486	0.542	-0.335	-0.374	-1.274	-1.420

Table 2: Ratio r [in 10^{-3} units] of the momentum observables at $\sqrt{s} = 500$ GeV for three different channels: $t + \bar{t} \rightarrow a(\mathbf{q}_+) + \bar{c}(\mathbf{q}_-) + X$, given the Set #2 of MSSM parameters. The left column includes only the t (W)EDFF corrections and the right one comes from the complete one-loop cross section for $e^+e^- \rightarrow t\bar{t}$.

3.2.6 Polarized beams

The previous results were obtained for unpolarized electron and positron beams. Let P_{\pm} be the degree of longitudinal polarization of the initial e^{\pm} . The differential cross section reads now

$$d\sigma = \frac{1}{4} [(1 + P_+)(1 + P_-) d\sigma_R + (1 - P_+)(1 - P_-) d\sigma_L], \quad (34)$$

where $\sigma_{R/L}$ corresponds to the cross section for electrons and positrons with equal right/left-handed helicity. Chirality conservation suppresses opposite helicities. Table 3 summarizes some extreme cases. If both beams are fully polarized, $P_+ = P_- = \pm 1$, the ratio r is the same as for $(P_{\pm} = 0, P_{\mp} = \pm 1)$, respectively, but the cross sections are twice as much (34), which results in a higher statistical significance of the CP signal. From comparison of Table 2 (right columns) with Table 3 is clear that left-handed polarized beams enhance the sensitivity to CP-violating effects.

$P_{\pm} = 0, P_{\mp} = -1; \sigma_{t\bar{t}} = 0.707 \text{ pb}$				$P_{\pm} = 0, P_{\mp} = +1; \sigma_{t\bar{t}} = 0.355 \text{ pb}$			
\mathcal{O}	$b - b$	$\ell - b$	$\ell - \ell$	\mathcal{O}	$b - b$	$\ell - b$	$\ell - \ell$
\hat{A}_1	0.359	-0.298	-0.667	\hat{A}_1	0.016	-0.009	-0.053
\hat{A}_2	0.397	-0.254	-0.952	\hat{A}_2	0.134	-0.099	-0.468
\hat{T}_{33}	0.065	-0.214	0.383	\hat{T}_{33}	-0.003	0.006	-0.020
\hat{Q}_{33}	0.708	-0.488	-1.848	\hat{Q}_{33}	0.210	-0.145	-0.555

Table 3: The same as in Table 2 assuming the complete one-loop cross section for $e^+e^- \rightarrow t\bar{t}$ and longitudinal polarizations for one of the e^{\pm} beams, P_{\pm} .

Concerning the experimental reach of this analysis, the statistical significance of the signal of CP violation is given by $N_{SD} = |r|\sqrt{N}$ with $N = \epsilon \mathcal{L} \sigma_{t\bar{t}} \text{BR}(t \rightarrow a) \text{BR}(\bar{t} \rightarrow \bar{c})$ where ϵ is the detection efficiency and \mathcal{L} the integrated luminosity of the collider. The branching ratios of the t decays are $\text{BR} \simeq 1$ for the b channel and $\text{BR} \simeq 0.22$ for the leptonic channels ($\ell = e, \mu$). At $\sqrt{s} = 500 \text{ GeV}$ the total cross section for t -pair production is $\sigma_{t\bar{t}} \simeq 0.5 \text{ pb}$. Assuming a LC integrated luminosity $\mathcal{L} \simeq 500 \text{ fb}^{-1}$ and a perfect detection efficiency, one gets $\sqrt{N} \simeq 500, 235, 110$ for the channels $b - b$, $\ell - b$, $\ell - \ell$, respectively. With these statistics, values of $|r| \sim 2 \times 10^{-3}, 4 \times 10^{-3}, 9 \times 10^{-3}$ for the channels above would be necessary to achieve a 1 s.d. effect. Such values can be hardly reached in the context of the MSSM for the given luminosity, even for polarized beams, as Tables 2 and 3 show.

4 Conclusions

In summary, the top-quark is an excellent laboratory to test the MSSM. If SUSY is realized in nature around the electroweak scale, the top-quark phenomenology differs significantly from the SM one. The various top-quark observables can be well investigated

at TESLA. The production cross-section receives radiative corrections that can be used to test the MSSM, or to derive bounds on the masses of the various sparticles. Also, in the MSSM there exist new sources of CP-violation effects, giving rise to specific CP-violating asymmetries in top-pair production, which, however, might be too small for being observable with the currently expected luminosity. The top-quark decay modes can differ significantly from the SM ones; of special importance is the $t \rightarrow H^+ b$ decay mode. Even in the case that the new particles of the MSSM are heavier than the top-quark, their virtual quantum effects influence the top-quark standard decay mode. Moreover, the LC presents a great sensitivity to the possible rare decays. In the MSSM some of these decays are strongly enhanced with respect to the SM expectations, and could be detected.

Acknowledgments

This work has been partially supported by the Deutsche Forschungsgemeinschaft, by CICYT under projects AEN99-0766 and AEN96-1672 and by Junta de Andalucía under project FQM-101.

References

- [1] H. P. Nilles, *Phys. Rept.* **110** (1984) 1;
 H. E. Haber, G. L. Kane, *Phys. Rept.* **117** (1985) 75;
 A. B. Lahanas, D. V. Nanopoulos, *Phys. Rept.* **145** (1987) 1;
 S. Ferrara, ed., *Supersymmetry*, vol. 1-2. North Holland/World Scientific, Singapore, 1987.
- [2] S. Snyder (D0 Collaboration), talk at the International Europhysics Conference on High Energy Physics (EPS99) 15-21 July 1999, Tampere, Finland.
- [3] J. Guasch, J. Solà, *Z. Phys.* **C74** (1997) 337–354, [hep-ph/9603441](#).
- [4] F. Abe *et al.* (CDF Collaboration), *Phys. Rev. Lett.* **79** (1997) 1992–1997; *ibid.* **80** (1998) 2767–2772, [hep-ex/9801014](#); *ibid.* **82** (1999) 271–276, [hep-ex/9810029](#), *erratum: ibid.* **82** (1999) 2808–2809;
 B. Abbott *et al.* (D0 Collaboration), *Phys. Rev.* **D58** (1998) 052001, [hep-ex/9801025](#); *ibid.* **D60** (1999) 052001, [hep-ex/9808029](#); *Phys. Rev. Lett.* **83** (1999) 1908, [hep-ex/9901023](#).
- [5] T. Teubner, talk at the Vth Workshop in the 2nd ECFA/DESY Study on Physics and Detectors for a Linear Electron-Positron Collider, Obernai (France) 16-19th October, 1999; K. Fujii, T. Matsui, Y. Sumino, *Phys. Rev.* **D50** (1994) 4341–4362;
 A. H. Hoang *et al.*, [hep-ph/0001286](#). Contribution to the Proceedings of the 2nd joint ECFA/DESY Workshop on Physics Studies for a Future Linear Collider.
- [6] M. Jeżabek, J. H. Kühn, *Nucl. Phys.* **B314** (1989) 1;
 M. Jeżabek, J. H. Kühn, *Nucl. Phys.* **B320** (1989) 20;
 C. S. Li, R. J. Oakes, T. C. Yuan, *Phys. Rev.* **D43** (1991) 3759–3762;
 A. Denner, T. Sack, *Nucl. Phys.* **B358** (1991) 46–58;
 K. G. Chetyrkin, R. Harlander, T. Seidensticker, M. Steinhauser, *Phys. Rev.* **D60** (1999) 114015, [hep-ph/9906273](#).

- [7] G. Eilam, R. R. Mendel, R. Migneron, A. Soni, *Phys. Rev. Lett.* **66** (1991) 3105–3108.
- [8] B. A. Irwin, B. Margolis, H. D. Trottier, *Phys. Lett.* **B256** (1991) 533–539;
C. P. Yuan, T.-C. Yuan, *Phys. Rev.* **D44** (1991) 3603–3609.
- [9] D. Garcia, W. Hollik, R. A. Jiménez, J. Solà, *Nucl. Phys.* **B427** (1994) 53–80,
[hep-ph/9402341](#).
- [10] A. Dabelstein, W. Hollik, C. Jünger, R. A. Jiménez, J. Solà, *Nucl. Phys.* **B454** (1995) 75–85, [hep-ph/9503398](#).
- [11] B. Grzadkowski, W. Hollik, *Nucl. Phys.* **B384** (1992) 101–112.
- [12] A. Denner, A. H. Hoang, *Nucl. Phys.* **B397** (1993) 483–501.
- [13] I. I. Y. Bigi, Y. L. Dokshitser, V. Khoze, J. Kühn, P. Zerwas, *Phys. Lett.* **B181** (1986) 157;
V. Barger, R. J. N. Phillips, *Phys. Rev.* **D41** (1990) 884;
A. C. Bawa, C. S. Kim, A. D. Martin, *Z. Phys.* **C47** (1990) 75–82;
M. Drees, D. P. Roy, *Phys. Lett.* **B269** (1991) 155–160;
B. K. Bullock, K. Hagiwara, A. D. Martin, *Phys. Rev. Lett.* **67** (1991) 3055–3057;
W. Bernreuther *et al.* Prepared for Workshops on Future e^+e^- Colliders, Hamburg, Germany, Sep 2-3, 1991 and Saariselka, Finland, Sep 9-14, 1991;
Z. Kunszt, F. Zwirner, *Nucl. Phys.* **B385** (1992) 3–75, [hep-ph/9203223](#);
D. P. Roy, *Phys. Lett.* **B283** (1992) 403–410.
- [14] A. Czarnecki, S. Davidson, *Phys. Rev.* **D47** (1993) 3063–3064, [hep-ph/9208240](#); *ibid.* **D48** (1993) 4183–4187, [hep-ph/9301237](#), and references therein.
- [15] J.-M. Yang, C.-S. Li, *Phys. Lett.* **B320** (1994) 117–122.
- [16] J. Guasch, R. A. Jiménez, J. Solà, *Phys. Lett.* **B360** (1995) 47–56, [hep-ph/9507461](#).
- [17] J. A. Coarasa, D. Garcia, J. Guasch, R. A. Jiménez, J. Solà, *Eur. Phys. J.* **C2** (1998) 373,
[hep-ph/9607485](#).
- [18] J. A. Coarasa, J. Guasch, J. Solà, W. Hollik, *Phys. Lett.* **B442** (1998) 326, [hep-ph/9808278](#).
- [19] G. 't Hooft, M. Veltman, *Nucl. Phys.* **B153** (1979) 365–401;
G. Passarino, M. Veltman, *Nucl. Phys.* **B160** (1979) 151.
- [20] J. A. Coarasa, R. A. Jiménez, J. Solà, *Phys. Lett.* **B406** (1997) 337–346, [hep-ph/9701392](#).
- [21] M. Carena, D. Garcia, U. Nierste, C. E. M. Wagner, [hep-ph/9912516](#).
- [22] R. Barbieri, G. F. Giudice, *Phys. Lett.* **B309** (1993) 86–90, [hep-ph/9303270](#);
R. Garisto, J. N. Ng, *Phys. Lett.* **B315** (1993) 372–378, [hep-ph/9307301](#);
M. A. Diaz, *Phys. Lett.* **B322** (1994) 207–212, [hep-ph/9311228](#);
F. M. Borzumati, *Z. Phys.* **C63** (1994) 291–308, [hep-ph/9310212](#);
S. Bertolini, F. Vissani, *Z. Phys.* **C67** (1995) 513–524, [hep-ph/9403397](#);
M. Carena, C. E. M. Wagner, *Nucl. Phys.* **B452** (1995) 45–79, [hep-ph/9408253](#).
- [23] J. Guasch, J. Solà, *Phys. Lett.* **B416** (1998) 353–360, [hep-ph/9707535](#).

- [24] G. Eilam, J. L. Hewett, A. Soni, *Phys. Rev.* **D44** (1991) 1473–1484, *erratum: ibid.* **D59** (1999) 039901;
B. Mele, S. Petrarca, A. Soddu, *Phys. Lett.* **B435** (1998) 401, [hep-ph/9805498](#).
- [25] C. S. Li, R. J. Oakes, J. M. Yang, *Phys. Rev.* **D49** (1994) 293–298, *erratum: ibid.* **D56** (1997) 3156;
G. Couture, C. Hamzaoui, H. König, *Phys. Rev.* **D52** (1995) 1713–1716, [hep-ph/9410230](#);
J. L. Lopez, D. V. Nanopoulos, R. Rangarajan, *Phys. Rev.* **D56** (1997) 3100–3106, [hep-ph/9702350](#);
G. Couture, M. Frank, H. König, *Phys. Rev.* **D56** (1997) 4213–4218, [hep-ph/9704305](#).
- [26] G. M. de Divitiis, R. Petronzio, L. Silvestrini, *Nucl. Phys.* **B504** (1997) 45, [hep-ph/9704244](#).
- [27] J. Guasch, J. Solà, *Nuc. Phys.* **B562** (1999) 3–28, [hep-ph/9906268](#).
- [28] J. Guasch, J. Solà, UAB-FT-473, KA-TP-15-1999, [hep-ph/9909503](#).
- [29] J.-M. Yang, C.-S. Li, *Phys. Rev.* **D49** (1994) 3412–3416, *erratum: ibid.* **D51** (1995) 3974.
- [30] J. M. Yang, B.-L. Young, X. Zhang, *Phys. Rev.* **D58** (1998) 055001, [hep-ph/9705341](#);
S. Bar-Shalom, G. Eilam, A. Soni, *Phys. Rev.* **D60** (1999) 035007, [hep-ph/9812518](#).
- [31] M. J. Duncan, *Nucl. Phys.* **B221** (1983) 285; *Phys. Rev.* **D31** (1985) 1139.
- [32] F. Gabbiani, E. Gabrielli, A. Masiero, L. Silvestrini, *Nucl. Phys.* **B477** (1996) 321–352, [hep-ph/9604387](#);
M. Misiak, S. Pokorski, J. Rosiek in *Heavy Flavours II*, A. Buras and M. Lindner, eds., Advanced Series on directions in High Energy Physics. World Scientific, Singapore, 1998, [hep-ph/9703442](#).
- [33] F. Borzumati, C. Greub, T. Hurth, D. Wyler, [hep-ph/9911245](#).
- [34] R. Frey *et al.*, FERMILAB-CONF-97-085, [hep-ph/9704243](#).
- [35] F. M. Borzumati, [hep-ph/9310348](#). Proc. of the Workshop Munich, Annecy, Hamburg, November 1992 to April 1993, P.M. Zerwas (Ed.), preprint DESY 93-123C, December 1993;
F. M. Borzumati, N. Polonsky, [hep-ph/9602433](#).
- [36] The LEP SUSY Working Group, (ALEPH, DELPHI, L3 and OPAL Collaborations), notes [LEPSUSYWG/98-04.1](#) and [LEPSUSYWG/98-04.1](#), <http://www.cern.ch/lepsusy/>.
- [37] L. Clavelli, [hep-ph/9908342](#).
- [38] A. Savoy-Navarro (CDF Collaboration), to be published in the proceedings of International Europhysics Conference on High-Energy Physics (EPS-HEP 99), Tampere, Finland, 15-21 July 1999.

[39] D. Garcia, J. Solà, *Phys. Lett.* **B354** (1995) 335–344, [hep-ph/9502317](#);
 J. D. Wells, C. Kolda, G. L. Kane, *Phys. Lett.* **B338** (1994) 219–228, [hep-ph/9408228](#);
 X. Wang, J. L. Lopez, D. V. Nanopoulos, *Phys. Rev.* **D52** (1995) 4116–4124, [hep-ph/9506217](#);
 A. Dabelstein, W. Hollik, W. Mösl, in: Proceedings of the Ringberg Workshop on *Perspectives for Electroweak Interactions in e^+e^- Collisions*, ed. B. A. Kniehl, World Scientific (1995), p. 345, [hep-ph/9506251](#);
 P. H. Chankowski, S. Pokorski, *Nucl. Phys.* **B475** (1996) 3–26, [hep-ph/9603310](#);
 W. de Boer, A. Dabelstein, W. Hollik, W. Mösl, U. Schwickerath, *Z. Phys.* **C75** (1997) 627, [hep-ph/9607286](#); [hep-ph/9609209](#).

[40] A. Djouadi, W. Hollik, C. Jünger, *Phys. Rev.* **D54** (1996) 5629–5635, [hep-ph/9605340](#).

[41] C. S. Li, R. J. Oakes, J. M. Yang, *Phys. Rev.* **D54** (1996) 6883–6889, [hep-ph/9606385](#);
 W. Beenakker, R. Höpker, T. Plehn, P. M. Zerwas, *Z. Phys.* **C75** (1997) 349, [hep-ph/9610313](#).

[42] A. Belyaev, J. Ellis, S. Lola, [hep-ph/0002220](#).

[43] W. Beenakker, S.C. van der Marck, W. Hollik, *Nucl. Phys.* **B365** (1991) 24.

[44] W. Beenakker, W. Hollik, *Phys. Lett.* **B269** (1991) 425;
 V. Driesen, W. Hollik, A. Kraft, [hep-ph/9603398](#), in: Proceedings of the Workshop on *Physics with e^+e^- Linear Colliders*, Annecy-Gran Sasso-Hamburg 1995, DESY 96-123D (1996), ed. P.M. Zerwas.

[45] A.A. Akhundov, D.Yu. Bardin, A. Leike, *Phys. Lett.* **B261** (1991) 321;
 A.B. Arbuzov, D.Yu. Bardin, A. Leike, *Mod. Phys. Lett.* **A7** (1992) 2029; *erratum: ibid.* **A9** (1994) 1515.

[46] W. Hollik, C. Schappacher, *Nucl. Phys.* **B545** (1999) 98, [hep-ph/9807427](#).

[47] W. Beenakker, A. Denner, A. Kraft, *Nucl. Phys.* **B410** (1993) 219;
 A. Denner, R.J. Guth, J. Kühn, *Nucl. Phys.* **B377** (1992) 3.

[48] J. Jerzak, E. Laermann, P.M. Zerwas, *Phys. Rev.* **D25** (1980) 1218;
 A. Djouadi, *Z. Phys.* **C39** (1988) 561;
 K. Chetyrkin, A. Hoang, J. Kühn, M. Steinhauser, T. Teubner, *Eur. Phys. J.* **C2** (1998) 137, [hep-ph/9711327](#);
 K. Chetyrkin, J. Kühn, M. Steinhauser, *Nucl. Phys.* **B482** (1996) 213, [hep-ph/9606230](#);
B505 (1997) 40, [hep-ph/9705254](#);
 K. Chetyrkin, R. Harlander, J. Kühn, M. Steinhauser, *Nucl. Phys.* **B503** (1997) 339, [hep-ph/9704222](#);
 R. Harlander, M. Steinhauser, *Eur. Phys. J.* **C2** (1998) 151, [hep-ph/9710413](#).

[49] J. Kühn, T. Hahn, R. Harlander, [hep-ph/9912262](#), to appear in the Proceedings of the Linear Collider Workshop, Sitges (Spain) 1999.

[50] S. Dimopoulos, S. Thomas, *Nucl. Phys.* **B465** (1996) 23, [hep-ph/9510220](#).

[51] W. Hollik, J.I. Illana, S. Rigolin, C. Schappacher, D. Stöckinger, *Nucl. Phys.* **B551** (1999) 3, *erratum: ibid.* **B557** (1999) 407, [hep-ph/9812298](#).

[52] W. Hollik, J.I. Illana, S. Rigolin, D. Stöckinger, *Phys. Lett.* **B416** (1998) 345, [hep-ph/9707437](#);
 B. de Carlos, J.M. Moreno, *Nucl. Phys.* **B519** (1998) 101, [hep-ph/9707487](#).

[53] W. Hollik, J.I. Illana, S. Rigolin, D. Stöckinger, *Phys. Lett.* **B425** (1998) 322, [hep-ph/9711322](#).

[54] J.F. Donoghue, *Phys. Rev.* **D18** (1978) 1632;
 E.P. Shabalin, *Sov. J. Nucl. Phys.* **28** (1978) 75;
 A. Czarnecki, B. Krause, *Phys. Rev. Lett.* **78** (1997) 4339.

[55] A. Bartl, E. Christova, W. Majerotto, *Nucl. Phys.* **B460** (1996) 235, *erratum: ibid.* **B465** (1996) 365, [hep-ph/9507445](#);
 A. Bartl, E. Christova, T. Gajdosik, W. Majerotto, *Nucl. Phys.* **B507** (1997) 35, *erratum: ibid.* **B531** (1998) 653, [hep-ph/9705245](#).

[56] W. Bernreuther, G.W. Botz, O. Nachtmann, P. Overmann, *Z. Phys.* **C52** (1991) 567;
 W. Bernreuther, O. Nachtmann, P. Overmann, T. Schröder, *Nucl. Phys.* **B388** (1992) 53, *erratum: ibid.* **B406** (1993) 516.

[57] W. Bernreuther, O. Nachtmann, *Phys. Rev. Lett.* **63** (1989) 2787, *erratum: ibid.* **64** (1990) 1072;
 W. Bernreuther, O. Nachtmann, P. Overmann, *Phys. Rev.* **D48** (1993) 78.

[58] S. Bar-Shalom, D. Atwood, A. Soni, *Phys. Rev.* **D57** (1998) 1495, [hep-ph/9708357](#);
 X. Bi, Y. Dai, *Eur. Phys. J.* **C12** (2000) 125, [hep-ph/9904228](#).

[59] A. Czarnecki, M. Jeżabek, J.H. Kühn, *Nucl. Phys.* **B351** (1991) 70.